Supplementary Information

Novel Tri-[2]rotaxane-based Stimuli-Responsive Fluorescent Nanoparticles and Its Guest Controlled Reversible Morphological Transformation Properties

Qi Lin*[a], Zhong-Hui Wang, Ting-Ting Huang, Tai-Bao Wei*, Hong Yao, You-Ming Zhang

Key Laboratory of Eco-Environment-Related Polymer Materials, Ministry of Education of China; Research Center of Gansu Military and Civilian Integration Advanced Structural Materials; College of Chemistry and Chemical Engineering, Northwest Normal University, Lanzhou, 730070, China; E-mail: linqi2004@126.com; weitaibao@126.com.

Contents

Materials 3
General procedure 3
Synthesis of Tri-pillar[5]arene **LTP** 4
Scheme S1 Syntheses of tri-pillar[5]arene acceptor **LTP** 4
Figure S1. ^{1}H NMR spectrum of compound **LTP** (DMSO-d_6, 400 MHz, 298 K). 5
Figure S2. ^{13}C NMR spectrum of compound **LTP** (DMSO-d_6, 150 MHz, 298 K). 5
Figure S3. FT-IR spectra of compound **LTP**. 6
Figure S4. Mass spectrum of compound **LTP**. 6
Figure S5. Photos showing the Tyndall effect of (a) tri-[2]pseudorotaxane and (b) tri-[2]rotaxane in solution. 6
Figure S6. 2D NOESY NMR spectrum of **LTP** and **DDA** (400 MHz, 298 K, $CDCl_3$) 7
Figure S7. Mass spectrum of compound **tri-[2]pseudorotaxane**.....7
Figure S8. Mass spectrum of compound **tri-[2]rotaxane**.....7
Figure S9. The energy-minimized structure of model **rotaxane**: (a) side view (b) top view. 8
Figure S10. The photograph of the fluorescent spectrum linear range for **G8.** 8
Figure S11. The fluorescence changes of tri-[2]rotaxane-based test papers after addition different concentration (from 1×10^{-1} M to 1×10^{-5} M) of suberic acid. 8
Figure S12. (a) fluorescence decay curves of tri-[2]rotaxane and tri-[2]rotaxane + **G8**; (b) fluorescence decay fitting curve of the tri-[2]rotaxane; (c) fluorescence decay fitting curve of tri-[2]rotaxane + **G8**. All the experiments were carried out in DMSO solution. 9
Figure S13 SEM of tri-[2]rotaxane self-assemble into fluorescence nanoparticles in different concentration (a) 10^{-2} M; (b) 10^{-3} M; (c) 10^{-4} M; (d) 10^{-5} M. 10
Figure S14. The SEM of morphology change by the addition of a) hydrochloric acid; b) acetic acid; c) lauryl acid; d) terephthalic acid into nanoparticles system. 10
Figure S15. (a) SEM images of the nano-thin film; (b) the nano-thin film after the addition of competitive regent trimethylamine. 10
Figure S16. The SEM of morphology change by the addition of a) triethylamine; b) ammonium hydroxide; c) sodium hydroxide; d) methylamine into nanofilm system. 11
Theoretical data 11

Materials

Reagents and analytical apparat

All raw chemicals were purchased by business approach and used as supplied without further purification. The solvents were purchased from Aladdin Reagent (Shanghai) Co, Ltd, China and used in the whole experiments. Triple distilled water was used throughout the experiment. Melting point was measured by an X-4 digital melting-point apparatus (uncorrected). Mercury-600 spectrometer and Mercury-400 recorded nuclear magnetic resonance spectra. Mass spectra were recorded by a Bruker Esquire 6000 plus apparatus. Shimadzu RF-5301PC spectrofluorophotometer recorded the fluorescence spectra. The infrared spectra were performed on a Digilab FTS-3000 Fourier transform-infrared spectrophotometer. Scanning electron microscopy was obtained with JSM-6701F instrument. The fluorescent information of the supramolecular polymer was characterized using Laser Scanning Confocal Microscope (LSCM, Olympus Fluoview FV1200).

General procedure

Fluorescence titration experiments

The solution containing tri-[2]rotaxane was prepared in DMSO solution (0.1 mM, 2 mL). Then, various equivalents of guest suberic acid **G8** (0.1 M) were added into the tri-[2]rotaxane solution and the fluorescence spectra were recorded.

^{1}H NMR titration of **LTP** toward **DDA** and **NL**

The **LTP** (8.0 mg) was dissolved in the $CDCl_3$ (600 μL). Afterwards, 1-3 equiv. of **DDA** was added into the $CDCl_3$ solution and the ^{1}H NMR spectra were recorded. Subsequently, corresponding equivalents of **NL** were added into previous mixed system respectively.

^{1}H NMR titration of the tri-[2]rotaxane toward **G8**

The tri-[2]rotaxane was prepared in the $CDCl_3$ (600 μL). Then, the guest **G8** (1 equiv.) was added into the tri-[2]rotaxane system and the ^{1}H NMR spectra were recorded.

Synthesis of Tri-pillar[5]arene **LTP**

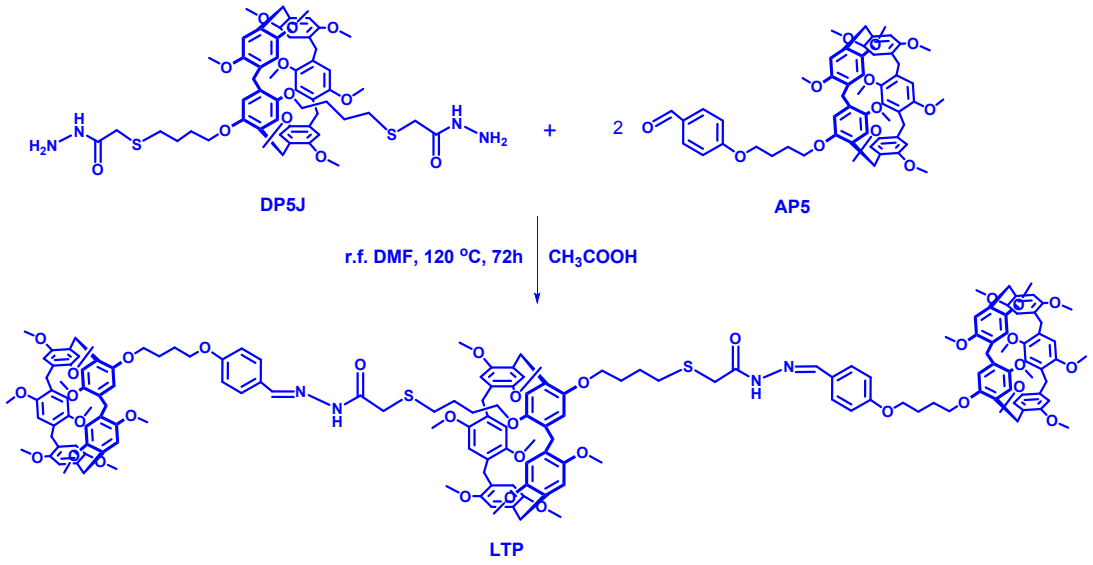

Scheme S1 Syntheses of tri-pillar[5]arene acceptor **LTP**

As shown in Scheme S1, The linear tri-pillar[5]arene **LTP** was successfully synthesized and characterized by ^{1}H NMR, ESI-MS, ^{13}C NMR and FT-IR spectra (Figure S1-S4). The intermediate compounds **DP5J** and **AP5** were reported according to our previous work[1,2], Initially, the novel linear acceptor (**LTP**) was successfully synthesized (Scheme 1) and fully characterized by ^{1}H NMR, ^{13}C NMR, FT-IR spectra and ESI-MS (Figure S1-S4). The **DP5J** (0.10 mmol, 0.10 g), **AP5** (0.25 mmol, 0.23 g) were added to DMF (20 mL), and the acetic acid (0.5 mL, as a catalyst) also was added to the mixtures as catalyst. Then reactants were stirred at 120 °C for 72 h. The solvent was evaporated and the solid was washed with anhydrous ethanol. The residue was dissolved in dichloromethane, then, purified by column chromatography (silica gel; petroleum ether/ethyl acetate = 2/1) and obtained white solid (0.06 g, 21 %). Mp: 125-127 °C. ^{1}H NMR (400MHz, DMSO-d_6) δ (ppm) :11.36 (s, 1H), 11.27 (s, 1H), 8.13 (s, 1H), 7.94 (s, 1H), 7.63-7.58 (m, 4H), 7.00-6.94 (m, 4H), 6.81-6.75 (m, 30H), 4.09-4.03 (m, 4H), 3.88 (s, 8H), 3.64 (s, 108H), 3.31 (s, 4H), 2.72 (s, 4H), 1.94-1.82 (m, 16H) (Figure. S1). ^{13}C NMR (DMSO-d_6, 151 MHz), δ/ppm: 162.63, 162.23, 150.86, 149.39, 147.12, 144.14, 129.80, 129.03, 128.02, 126.29, 114.92, 113.93, 112.66, 68.50, 56.13, 44.23, 33.83, 29.60, 28.64, 27.88, 26.15 (Figure. S2). FT-IR (anhydrous KBr, cm^{-1}) v: 3439 (N-H), 2929 (C-H), 1683 (C=O) and 1502 (C=N) (Figure. S3). ESI-MS m/z: calcd

for $C_{165}H_{186}N_4O_{34}S_2$, [M]: 2832.24; found 2832.25 (Figure. S4).

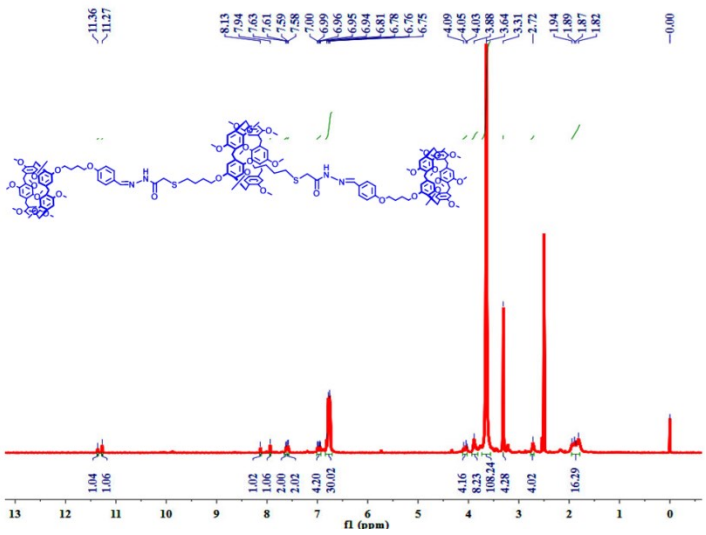

Figure S1. ^{1}H NMR spectrum of compound **LTP** (DMSO-d_6, 400 MHz, 298 K).

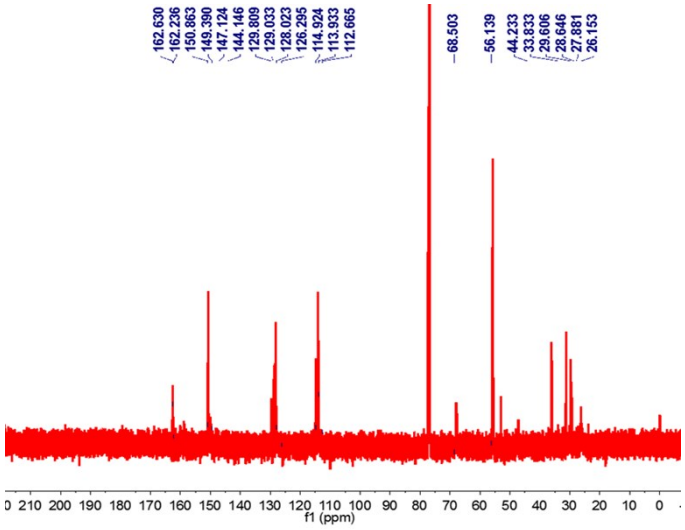

Figure S2. ^{13}C NMR spectrum of compound **LTP** (DMSO-d_6, 150 MHz, 298 K).

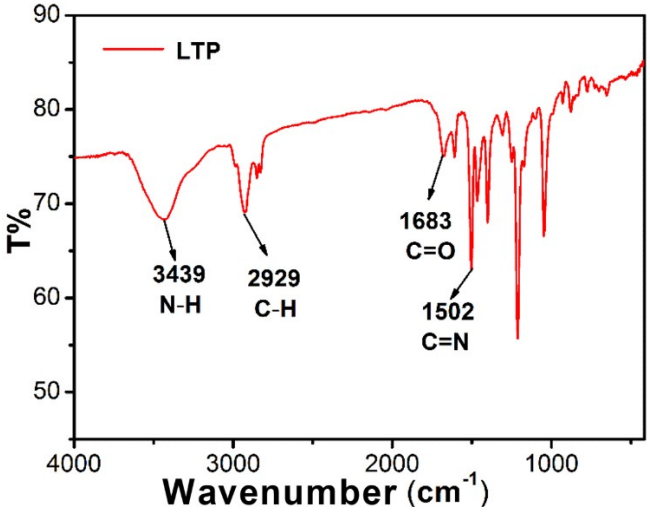

Figure S3. FT-IR spectra of compound **LTP**.

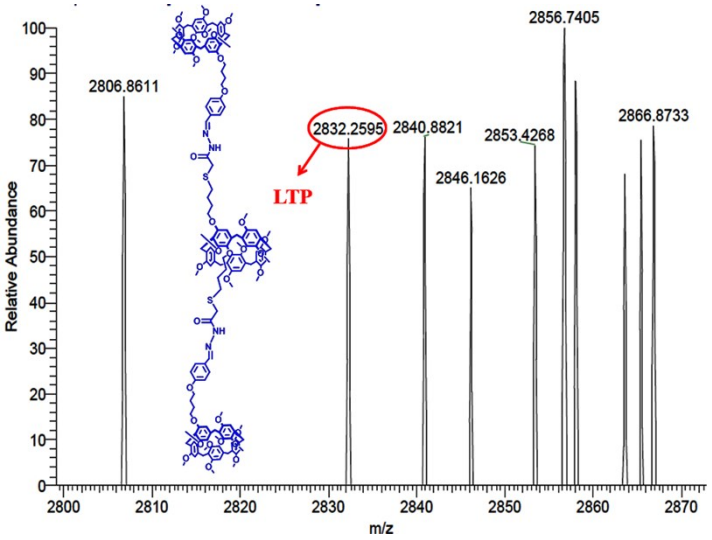

Figure S4. Mass spectrum of compound **LTP**.

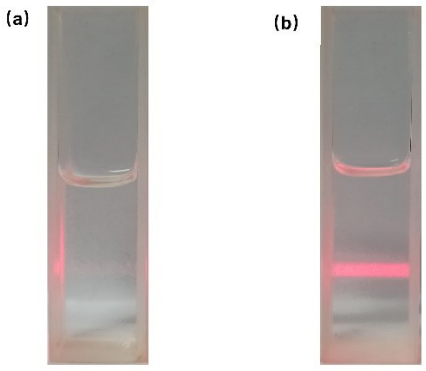

Figure S5. Photos showing the Tyndall effect of (a) tri-[2]pseudorotaxane and (b) tri-[2]rotaxane in solution.

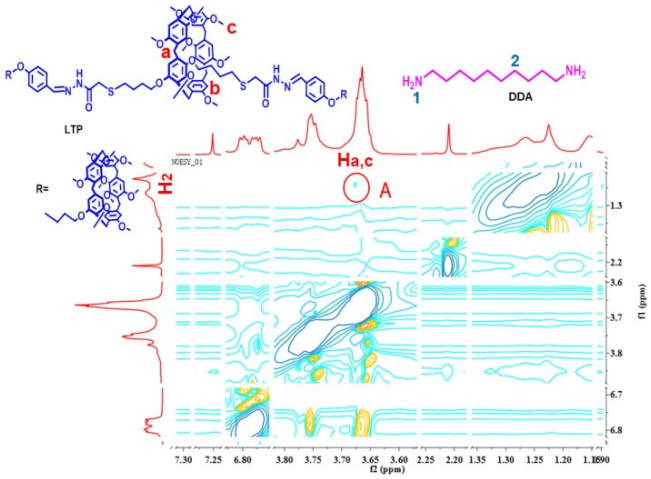

Figure S6. 2D NOESY NMR spectrum of **LTP** and **DDA** (400 MHz, 298 K, $CDCl_3$)

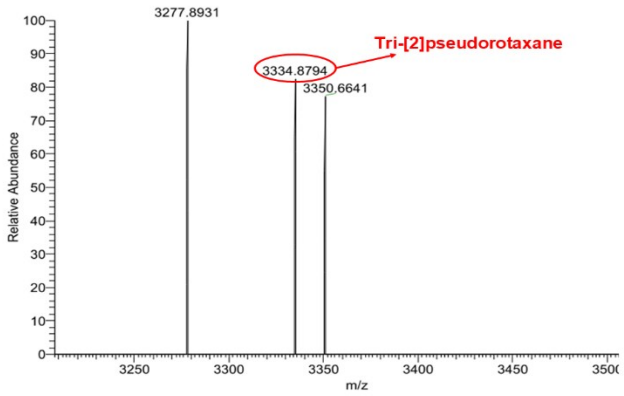

Figure S7. Mass spectrum of compound **tri-[2]pseudorotaxane**.

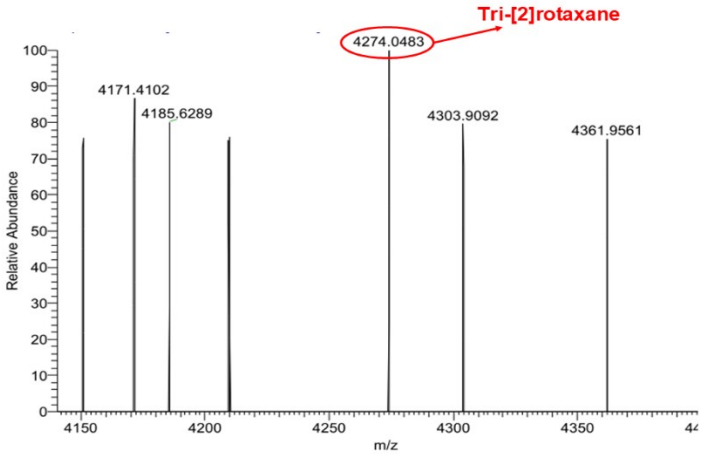

Figure S8. Mass spectrum of compound **tri-[2]rotaxane**.

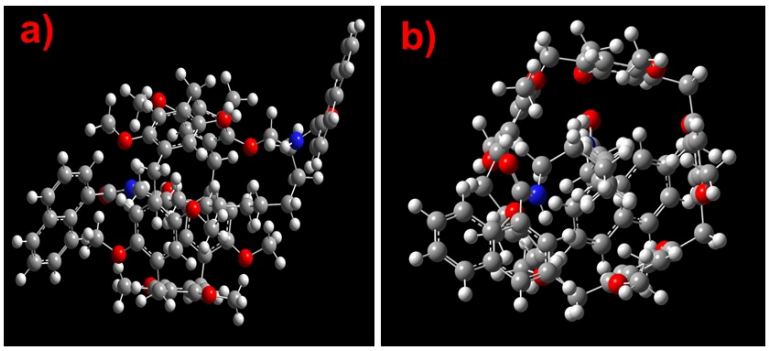

Figure S9. The energy-minimized structure of model **rotaxane**: (a) side view (b) top view.

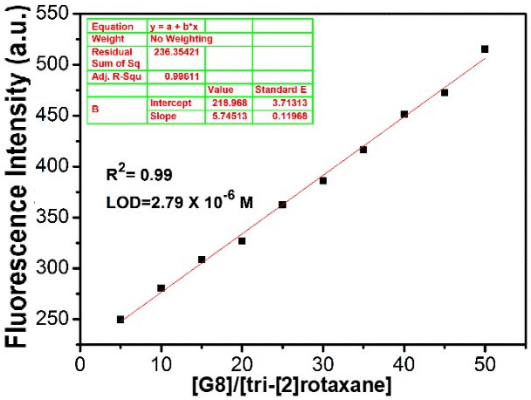

Figure S10. The photograph of the fluorescent spectrum linear range for **G8.**

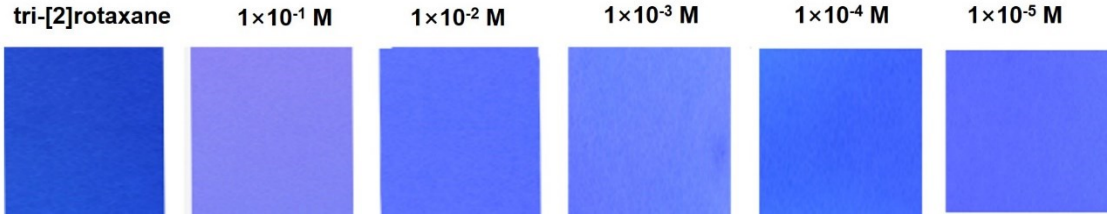

Figure S11. The fluorescence changes of tri-[2]rotaxane-based test papers after addition different concentration (from 1×10^{-1} M to 1×10^{-5} M) of suberic acid.

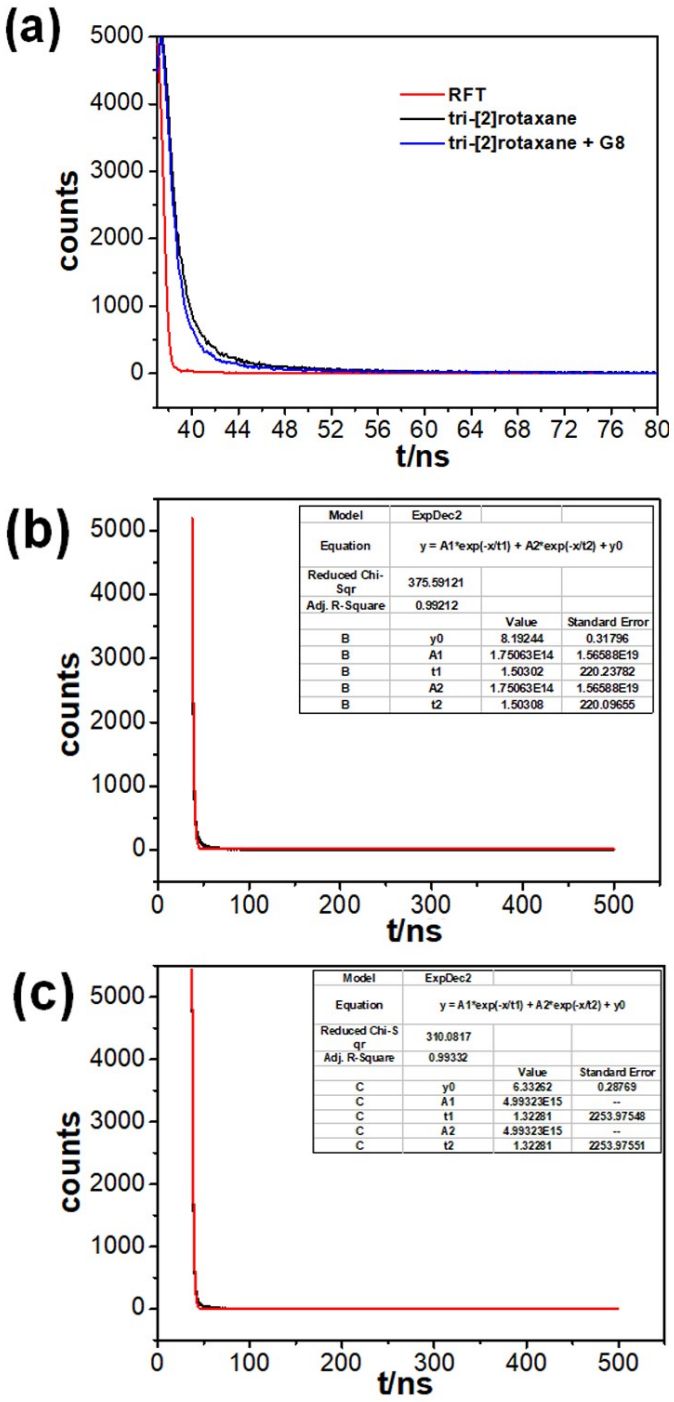

Figure S12. (a) fluorescence decay curves of tri-[2]rotaxane and tri-[2]rotaxane + **G8**; (b) fluorescence decay fitting curve of the tri-[2]rotaxane; (c) fluorescence decay fitting curve of tri-[2]rotaxane + **G8**. All the experiments were carried out in DMSO solution.

$$\bar{t} = A_1t_1^2 + A_2t_2^2 + A_3t_3^2 \,/\, A_1t_1 + A_2t_2 + A_3t_3 \quad \text{(S1)}$$

$$\varphi = \frac{{n_f}^2 A_s D_f}{{n_s}^2 A_f D_s} \varphi_s \qquad (A \leq 0.05) \qquad (S2)$$

Where A represents the absorbance, n represents the refractive index of the solution, and D represents the corrected fluorescence emission spectral integral area. Excitation was chosen at 365 nm. Among which $n_f = n_s$, $\varphi_{f1} = (820 \times 0.01) / (1147 \times 0.046) \times 0.55 = 0.08$; $\varphi_{f2} = (1380 \times 0.01) / (1147 \times 0.025) \times 0.55 = 0.26$;

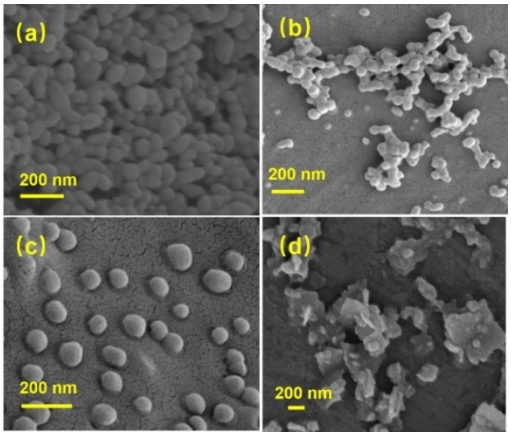

Figure S13 SEM of tri-[2]rotaxane self-assemble into fluorescence nanoparticles in different concentration (a) 10^{-2} M; (b) 10^{-3} M; (c) 10^{-4} M; (d) 10^{-5} M.

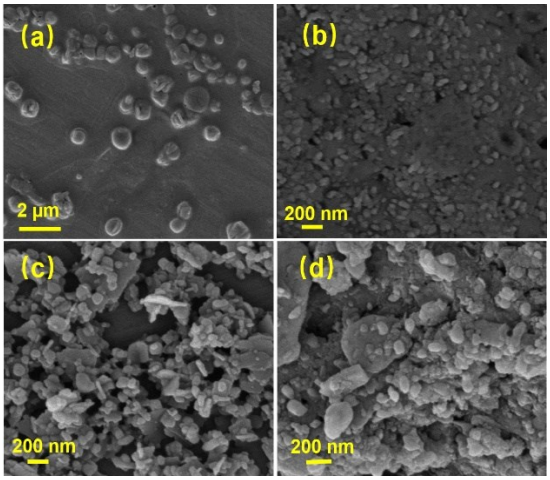

Figure S14. The SEM of morphology change by the addition of a) hydrochloric acid; b) acetic acid; c) lauryl acid; d) terephthalic acid into nanoparticles system.

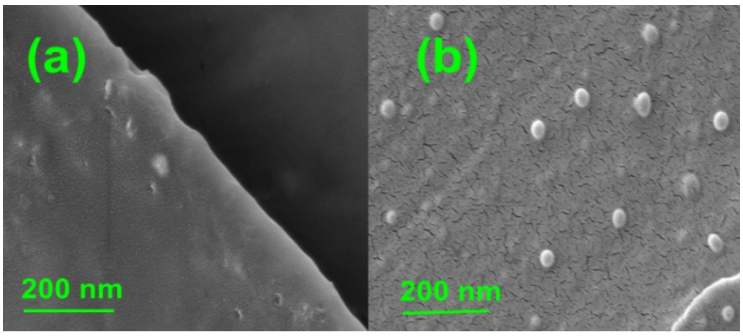

Figure S15. (a) SEM images of the nano-thin film; (b) the nano-thin film after the addition of competitive regent trimethylamine.

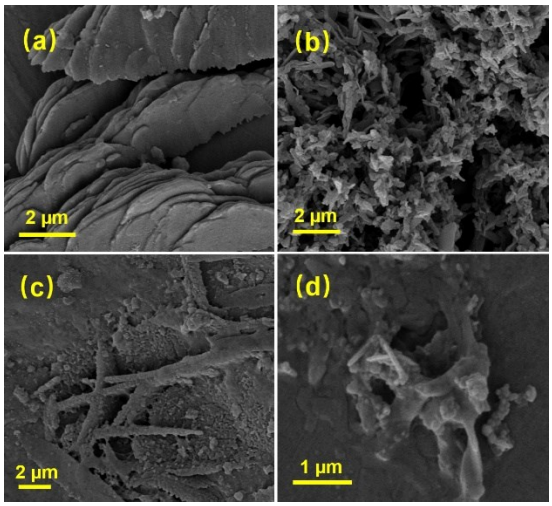

Figure S16. The SEM of morphology change by the addition of a) triethylamine; b) ammonium hydroxide; c) sodium hydroxide; d) methylamine into nanofilm system.

[1] Q. Lin, Y.Q. Fan, G.F. Gong, P.P. Mao, J. Wang, X.W. Guan, J. Liu, Y.-M. Zhang, H. Yao, T.-B. Wei, ACS Sustain Chem. Eng. 2018, 6, 8775-8781.

[2] T.-B. Wei, J.D. Ding, J.F. Chen, B.B. Han, X.M. Jiang, H. Yao, Y.-M. Zhang, Q. Lin, *New J. Chem*, 2018, **42**, 1271-1275.

Theoretical data

Sim-**[2]rotaxane**

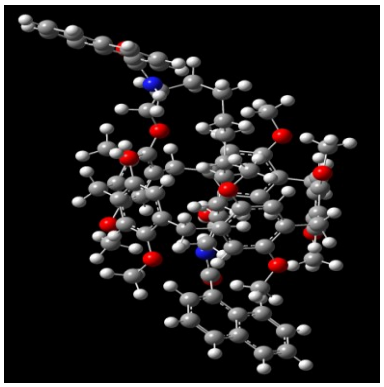

C	2.51444	-3.83249	1.19867
C	3.22923	-3.84288	-0.00072
C	2.60575	-4.14432	-1.20676
C	1.22546	-4.42344	-1.20616
C	0.51402	-4.41757	-0.00871
C	1.15397	-4.1398	1.20703
C	3.35974	-4.06441	-2.52404
H	2.91149	-4.76131	-3.23537
H	4.40694	-4.33095	-2.36394
C	3.29228	-2.64987	-3.08097
C	2.26313	-2.26053	-3.9402
C	4.24859	-1.70146	-2.6907
C	2.19567	-0.95809	-4.43977
C	4.18243	-0.4007	-3.19099
C	3.17335	-0.02055	-4.07639
C	3.10227	1.40048	-4.61191
H	2.65974	1.37962	-5.61045
H	4.11059	1.81645	-4.67299
C	2.26092	2.28284	-3.70385
C	2.85761	2.9464	-2.62099
C	0.88678	2.41418	-3.90677
C	2.07799	3.74501	-1.7819
C	0.10838	3.21395	-3.06891

C	0.70785	3.89798	-2.00255
C	-0.15159	4.7408	-1.07165
H	0.44228	5.5612	-0.66288
H	-0.99218	5.14638	-1.63868
C	-0.6706	3.88587	0.07219
C	0.10636	3.73275	1.23549
C	-1.86676	3.18362	-0.02631
C	-0.31609	2.88373	2.25445
C	-2.30374	2.35104	1.00667
C	-1.53084	2.19019	2.15716
C	-1.95472	1.23414	3.2608
H	-1.62188	1.62145	4.2273
H	-3.04369	1.15043	3.26261
C	-1.35486	-0.14904	3.05468
C	-0.07962	-0.45887	3.56361
C	-2.04631	-1.13204	2.35214
C	0.44944	-1.73702	3.38989
C	-1.51191	-2.40693	2.16592
C	-0.2645	-2.72825	2.70542
C	0.35447	-4.10138	2.49832
H	-0.43253	-4.85817	2.45765
H	1.02035	-4.32577	3.33472
H	-0.55768	-4.56059	0.01492
H	-3.00797	-0.88707	1.92293
H	1.5	-2.99293	-4.16313
H	-2.42595	3.24366	-0.95087
H	0.44601	1.83297	-4.70435
H	2.49985	4.2304	-0.91311
H	4.87855	0.3627	-2.87392

H	0.29594	2.6962	3.12475
H	1.44103	-1.98716	3.74159
H	4.26487	-3.53043	-0.02427
O	-2.23179	-3.37459	1.41023
O	3.12512	-3.40698	2.40745
O	0.65515	-4.67489	-2.45531
O	5.21601	-2.14223	-1.77971
O	1.19216	-0.49758	-5.30258
O	4.23439	2.7465	-2.46009
O	-1.27588	3.38169	-3.20499
O	1.29778	4.46305	1.27143
O	-3.52469	1.6319	0.87362
C	-3.27844	-4.06446	2.20374
H	-4.01098	-3.34801	2.58924
H	-2.83342	-4.61439	3.0404
C	4.35178	-4.14886	2.83558
H	5.11467	-3.39241	3.02814
H	4.10895	-4.7201	3.73598
H	4.67505	-4.82866	2.04272
C	-0.77143	-4.98919	-2.49172
H	-1.37528	-4.1444	-2.14268
H	-0.98927	-5.19492	-3.54055
H	-1.00242	-5.87398	-1.88654
C	6.27157	-1.20434	-1.40677
H	5.86974	-0.33437	-0.8754
H	6.92688	-1.76214	-0.73853
H	6.83507	-0.86372	-2.28353
C	0.12662	-1.43106	-5.64723
H	-0.43708	-1.7407	-4.75848

H	-0.52669	-0.88033	-6.32558
H	0.51555	-2.32216	-6.15501
C	4.87641	3.37079	-1.30831
H	4.46575	2.99476	-0.36348
H	5.92909	3.09534	-1.38092
H	4.77768	4.46295	-1.33224
C	-1.91764	2.76488	-4.35999
H	-1.8697	1.67091	-4.30876
H	-2.95864	3.08762	-4.31297
H	-1.46672	3.10332	-5.30081
C	2.07945	4.40998	2.50096
H	2.45745	3.3989	2.69266
H	2.91621	5.09001	2.33584
H	1.49294	4.74368	3.36541
C	-4.72475	2.48916	1.02206
H	-4.7249	3.29164	0.27697
H	-5.57711	1.82685	0.86619
H	-4.76662	2.92844	2.0247
O	0.59245	0.57317	4.22686
C	1.77778	0.2104	5.01378
H	2.60794	-0.09604	4.36878
H	1.54833	-0.59239	5.72367
C	-3.4432	-0.49379	-2.02592
C	-2.04624	-1.11529	-1.79107
H	-3.62168	0.25313	-1.24219
H	-3.43876	0.0417	-2.98595
C	-0.98744	-0.05378	-1.41961
H	-2.09664	-1.8393	-0.96725
H	-1.73271	-1.66785	-2.69044

C	0.36379	-0.69037	-1.0354
H	-0.85327	0.66559	-2.23696
H	-1.36646	0.50924	-0.5601
H	0.16235	-1.54705	-0.37983
H	0.87577	-1.07579	-1.92393
C	3.18013	0.31641	1.48142
H	2.43546	0.77503	2.14422
H	3.79183	1.10643	1.0421
H	3.69461	-1.56047	2.35969
N	4.05875	-0.59666	2.27322
C	1.2973	0.28143	-0.27419
C	2.45138	-0.49535	0.39435
H	0.71234	0.78789	0.50414
H	1.68495	1.04902	-0.95229
H	2.02564	-1.38243	0.87142
H	3.17043	-0.84555	-0.35254
C	-4.87383	-2.15769	-0.64081
C	-5.39962	-1.12689	0.38221
H	-3.96362	-2.60218	-0.22119
H	-5.62358	-2.95202	-0.74798
H	-5.66608	-1.62555	1.31792
H	-4.64669	-0.36056	0.58346
H	-6.59345	0.21226	-0.8143
C	-11.32832	0.6267	2.81006
C	-10.24525	0.16365	2.09814
C	-10.15184	0.38158	0.69237
C	-11.2268	1.07525	0.03639
C	-12.32846	1.54	0.80766
C	-12.37773	1.32637	2.16501

H	-11.38556	0.44769	3.87764
H	-9.4587	-0.40757	2.56788
C	-9.02799	-0.04116	-0.09645
C	-11.17818	1.27548	-1.36994
H	-13.13068	2.06519	0.29999
H	-13.22105	1.68404	2.74436
C	-10.11469	0.81352	-2.1083
C	-9.04002	0.15883	-1.46615
H	-12.0038	1.78933	-1.85086
H	-10.09304	0.94532	-3.1836
H	-8.22412	-0.22294	-2.06903
C	9.9434	1.45462	0.85491
C	9.19688	2.53691	1.25674
C	7.89558	2.36233	1.80646
C	7.35437	1.03583	1.92659
C	8.16927	-0.06402	1.52583
C	9.42487	0.14411	1.00155
H	7.56464	4.46673	2.18049
H	10.93398	1.59745	0.43914
H	9.59012	3.54418	1.1679
C	7.13405	3.47401	2.25923
C	6.01699	0.88277	2.43157
H	7.78342	-1.05734	1.70014
H	10.03389	-0.70439	0.71112
C	5.32897	1.99405	2.88327
C	5.88592	3.2909	2.80631
H	4.34338	1.86667	3.31306
H	5.32141	4.13733	3.17955
C	5.39124	-0.48336	2.54549

O	6.07645	-1.48476	2.88719
C	-7.84784	-0.72624	0.54411
O	-7.9257	-1.44938	1.56017
N	-6.64282	-0.46374	-0.06227
C	-4.58025	-1.54536	-2.03254
H	-5.5065	-1.09357	-2.41549
H	-4.31747	-2.35285	-2.73009
H	-3.76286	-4.75516	1.5126
H	2.04267	1.11864	5.55713